Supporting Information for "Assessing the Effectiveness of Thin-Layer Sand Caps for Contaminated Sediment Management through Passive Sampling"

David J. Lampert[1], William V. Sarchet[2], and Danny D. Reible[3*]

Department of Civil, Architectural, Environmental Engineering, The University of Texas at Austin, 1 University Station C1786, Austin, TX 78712-0273

Summary

The supporting information for this manuscript contains tables of data for all measured polycyclic aromatic hydrocarbons (PAHs) in the passive samplers used this study, a photograph of the 4-cm cap microcosm at the beginning and end of the study, a figure with the dimensionless concentration profiles for all of the PAHs in the control, 2.5-cm capped, and 4.5-cm capped microcosms, a tabulated summary of the tissue concentrations in the 4-cm cap microcosms at 28 and 56 days, and support for a diffusion modeling approach in the control, 2.5, and 4.5-cm caps.

Tabulated PAH Pore Water Concentrations

The PAH passive sampling data are summarized by compound into seven tables (S.1 through S.7) across four pages. The values in these tables are mean concentrations based on three replicates at depths from -3 cm to 10 cm, where 0 corresponds to the

[1]Postdoctoral Fellow, The University of Texas at Austin, 1 University Station C1786, Austin, TX 78712-0273

[2] Staff Engineer, Carollo Engineers, 8911 N Capital of Texas # 2200, Austin, TX 78759

[3]Bettie Margaret Smith Chair of Environmental Health Engineering, Department of Civil, Architectural, Environmental Engineering, The University of Texas at Austin, 1 University Station C1786, Austin, TX 78712-0273, reible@mail.utexas.edu, phone: (512) 471-4642, fax: (512) 471-5870

sediment-water interface, negative values are in the overlying water, and positive values are in the sediment/sand.

S.1 Phenanthrene Pore Water Concentrations (ng/L) in Various Caps

Depth (cm)	Control	2-cm cap	4-cm cap	6-cm cap	10-cm cap
-3	21	27	27	1	0
-2	13	38	8	3	0
-1	10	17	10	0	0
0	11	28	8	0	9
1	91	67	36	3	35
2	121	107	117	46	62
3	141	181	163	176	96
4	155	179	199	266	136
5	174	180	166	214	121
6	193	193	175	130	118
7	173	202	182	161	116
8	173	204	187	178	126
9	NA	NA	NA	NA	117
10	NA	NA	NA	NA	129
11	NA	NA	NA	NA	132

S.2 Pyrene Pore Water Concentrations (ng/L) in Various Caps

Depth (cm)	Control	2-cm cap	4-cm cap	6-cm cap	10-cm cap
-3	73	38	36	7	0
-2	53	82	11	4	0
-1	47	62	19	25	0
0	106	184	8	2	0
1	716	526	234	58	26
2	1016	716	488	139	67
3	1101	1059	558	214	72
4	1211	1235	1016	365	86
5	1268	1370	1238	717	68
6	1377	1409	1369	1218	79
7	1248	1390	1354	1425	82
8	1199	1398	1339	1445	126
9	NA	NA	NA	NA	151
10	NA	NA	NA	NA	311
11	NA	NA	NA	NA	836

S.3 Chrysene Pore Water Concentrations (ng/L) in Various Caps

Depth (cm)	Control	2-cm cap	4-cm cap	6-cm cap	10-cm cap
-3	0	0	0	0	0
-2	0	0	0	0	0
-1	0	0	0	0	0
0	0	1.55	0	0	0
1	4.72	4.17	1.33	0	0
2	7.98	7.12	5.85	1.04	0
3	7.20	10.04	7.48	2.68	0
4	7.01	9.08	9.67	4.79	0
5	8.22	8.00	10.27	5.62	0
6	7.38	9.00	9.77	6.44	0
7	7.81	8.00	8.12	5.95	0
8	7.44	8.45	7.34	5.26	0
9	NA	NA	NA	NA	0.80
10	NA	NA	NA	NA	0.49
11	NA	NA	NA	NA	3.91

S.4 Benz[a]anthracene Pore Water Concentrations (ng/L) in Various Caps

Depth (cm)	Control	2-cm cap	4-cm cap	6-cm cap	10-cm cap
-3	0	0	0	0	0
-2	0	0	0	0	0
-1	0	0	0	0	0
0	0	4.2	0	0	0
1	8.0	7.7	5.2	0	0
2	13.2	10.8	9.4	1.2	0
3	13.5	16.1	11.3	2.0	0
4	13.6	16.8	14.8	4.9	1.6
5	14.4	17.3	18.8	8.8	2.1
6	14.3	16.9	20.0	12.9	1.8
7	14.8	15.8	18.0	14.4	1.6
8	14.1	16.1	16.6	12.9	3.8
9	NA	NA	NA	NA	3.9
10	NA	NA	NA	NA	5.6
11	NA	NA	NA	NA	10.8

S.5 Benzo[b]fluoranthene Pore Water Concentrations (ng/L) in Various Caps

Depth (cm)	Control	2-cm cap	4-cm cap	6-cm cap	10-cm cap
-3	0.70	1.15	0.16	0.05	0
-2	0.67	1.32	0.73	0	0
-1	0.63	1.04	0.44	0.05	0
0	0.98	2.82	0.67	0.09	0
1	2.51	2.85	1.85	0.29	0
2	3.86	3.58	1.79	0.60	0.74
3	3.65	4.99	2.20	1.52	0.00
4	4.09	4.89	4.05	2.06	0.36
5	4.39	4.58	7.05	2.55	0.23
6	4.68	4.19	5.85	3.41	0.63
7	4.16	3.94	4.07	3.99	0.44
8	4.03	4.12	3.26	3.05	0.73
9	NA	NA	NA	NA	1.10
10	NA	NA	NA	NA	1.29
11	NA	NA	NA	NA	2.65

S.6 Benzo[k]fluoranthene Pore Water Concentrations (ng/L) in Various Caps

Depth (cm)	Control	2-cm cap	4-cm cap	6-cm cap	10-cm cap
-3	0	0	0	0	0
-2	0	0.40	0.03	0	0
-1	0	0.14	0	0	0
0	0	0.99	0	0	0
1	0.56	0.85	0.42	0	0
2	1.13	1.27	0.49	0.03	0
3	0.96	1.89	0.64	0.33	0
4	1.08	1.69	1.36	0.17	0
5	1.09	1.41	2.26	0.35	0
6	1.08	1.41	1.70	0.40	0.03
7	1.01	1.18	1.08	0.68	0.02
8	0.85	1.20	0.87	0.28	0
9	NA	NA	NA	NA	0
10	NA	NA	NA	NA	0.21
11	NA	NA	NA	NA	0.56

S.7 Benzo[a]pyrene Pore Water Concentrations (ng/L) in Various Caps

Depth (cm)	Control	2-cm cap	4-cm cap	6-cm cap	10-cm cap
-3	0.18	0.48	0.03	0	0
-2	0.16	0.61	0.05	0	0
-1	0.05	0.59	0.05	0.08	0
0	0.28	1.46	0.01	0.04	0
1	1.29	1.24	0.47	0.06	0.08
2	2.09	1.77	0.44	0.06	0.15
3	1.92	2.28	0.43	0.20	0.25
4	1.97	2.43	0.95	0.20	0.33
5	2.13	2.25	1.91	0.49	0.20
6	2.10	2.37	1.35	0.90	0.28
7	2.00	1.94	1.23	1.27	0.18
8	1.68	2.18	1.37	1.06	0.33
9	NA	NA	NA	NA	0.41
10	NA	NA	NA	NA	0.73
11	NA	NA	NA	NA	1.15

Microcosm Photograph

The following photograph of the 4-cm cap microcosm at the beginning and end of the study that illustrates the effects and depth of bioturbation is presented in Figure S.1.

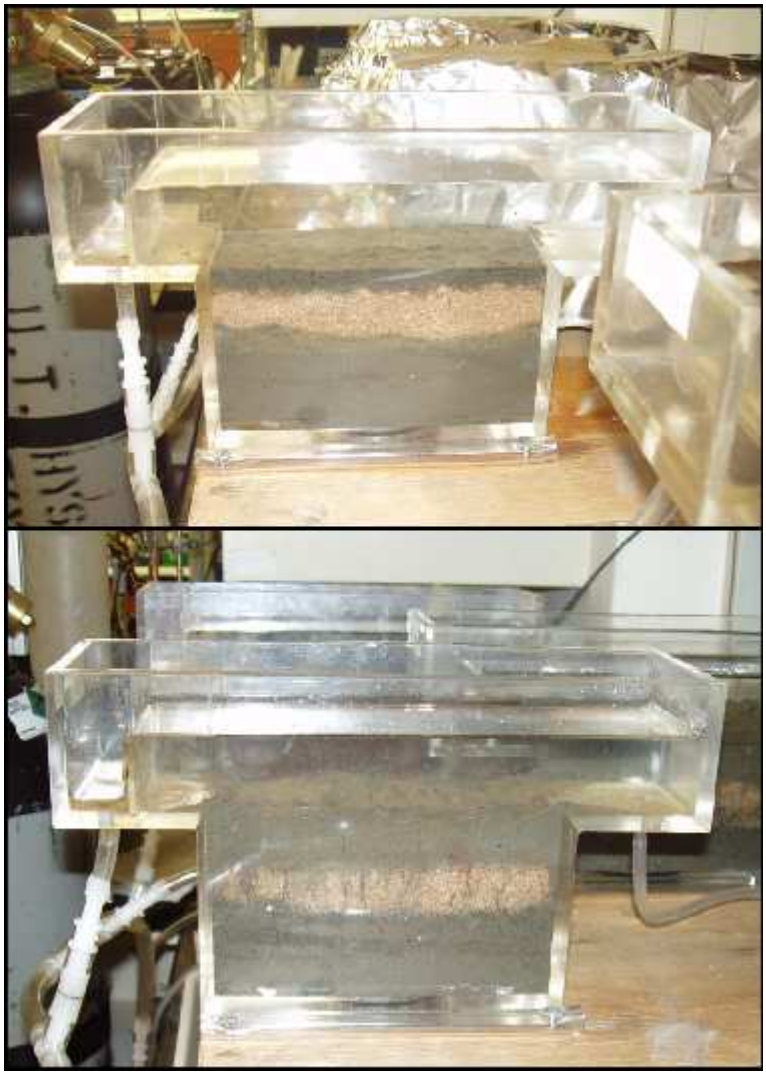

Figure S.1. 4-cm microcosm at time = 0 and time = 28 days. The effects of bioturbation to compromise the cap can be clearly seen in this microcosm. The depth of bioturbation was estimated to be 4.5 cm.

Dimensionless Profiles for Various PAHs

In Figure S.2 the dimensionless concentration profiles for all of the PAHs in the control, 2.5-cm capped, and 4.5-cm capped microcosms are plotted to illustrate the compound-independent effect of bioturbation on solute transport in this study.

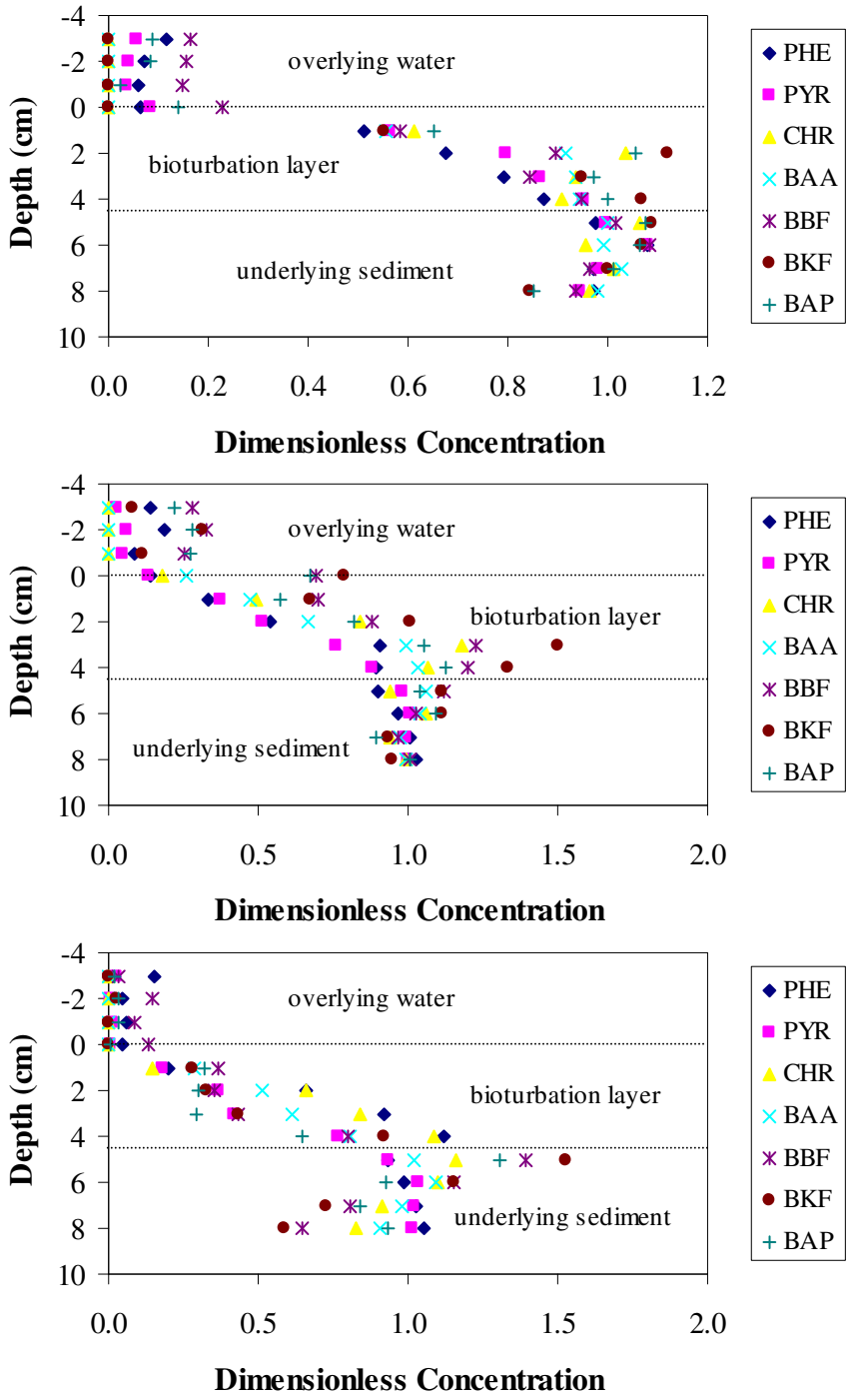

Figure S.2. Dimensionless concentration profiles for all compounds in control (top), 2.5-cm (middle), and 4.5 cm (bottom) capped cells. The effects of bioturbation were relatively compound-independent.

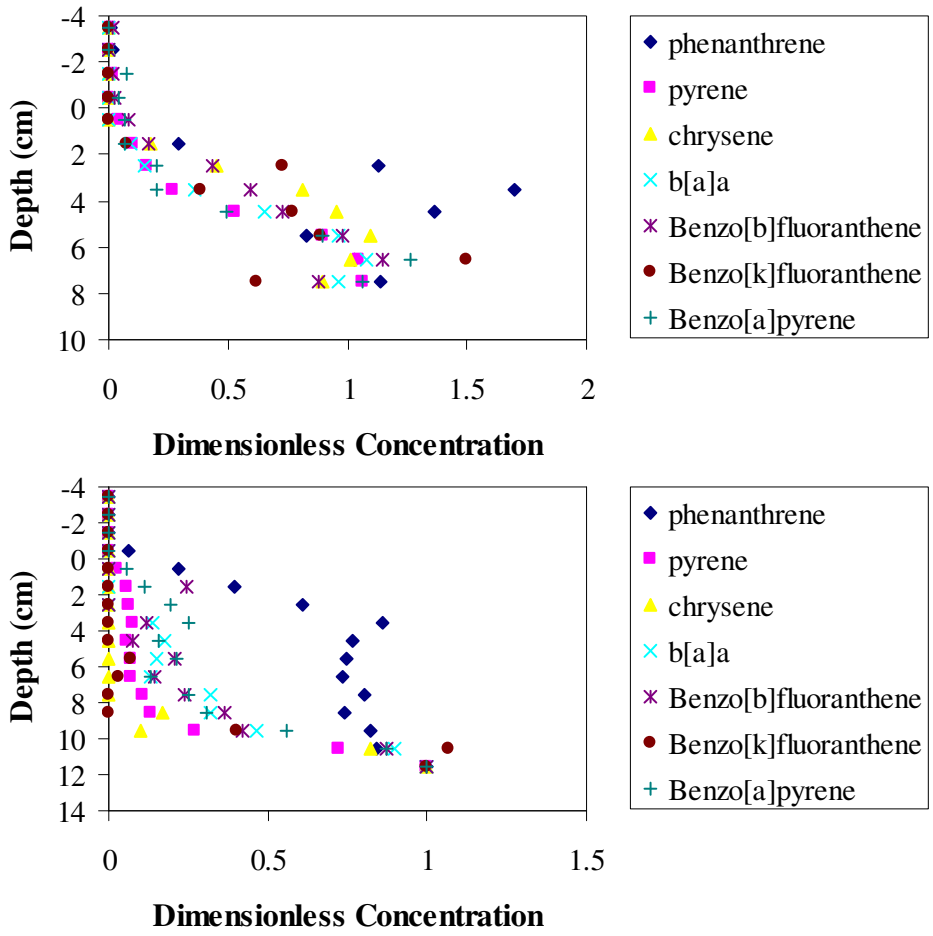

Figure S.3. Dimensionless concentration profiles for all compounds in 6.5-cm (top) and 10.5-cm (bottom) capped cells. Profiles were observed to be compound specific.

Worm Lipid and Tissue Concentrations

Table S.8 contains a summary of the tissue concentrations in the 4-cm cap microcosms at 28 and 56 days. Table S.9 contains the lipid fraction measurements for the microcosms and the percentage recovery of worms out of 250 initially.

Table S.8: Comparison of 28 and 56-Day Tissue Concentrations (Dry Weight) in 4-cm Microcosm

Compound	28-Day (ng/g) (Mean +/- Standard Deviation)	56-Day Concentration (ng/g) (Mean +/- Standard Deviation)
PHE	397 +/- 54	132 +/- 83
PYR	7491 +/- 1899	3877 +/- 1310
CHR	368 +/- 72	184 +/- 60
BAA	321 +/- 79	153 +/- 67
BBF	268 +/- 70	121 +/- 50
BKF	77 +/- 17	34 +/- 17
BAP	124 +/- 57	61 +/- 58

Table S.9: Worm lipid content (dry weight) and recovery percentage measurements

Cell	Lipid Fraction (%)	Percent Recovery
control	10.8	107
2.5-cm	6.8	83
4.5-cm	7.8	91
6.5-cm	8.6	92
10.5-cm	10.7	76

Modeling of Expected Dimensionless Profiles

The concentration profiles for the control, 2.5-cm, and 4.5-cm caps initially, at 28 days, and at steady state using a biodiffusion model with a coefficient D_{bio} = 3.1(10)$^{-7}$ cm^2/s are depicted along with the observed 28-day data in Figure S.4. The governing equation and boundary conditions for the pore water concentration C at time t and depth z

with an underlying concentration of C_0, a biodiffusion coefficient D_{bio} at depth L = 4.5 cm are the same for each case:

$$\frac{\partial C}{\partial t} = D_{bio}\frac{\partial^2 C}{\partial z^2} \tag{S.1}$$

$$C(z=0,t)=0 \tag{S.2}$$

$$C(z=L,t)=C_0 \tag{S.3}$$

The initial conditions for the control cell, the 2.5-cm cap cell, and the 4.5-cm cell are respectively:

$$C(z,t=0)=0 \tag{S.4}$$

$$C(z,t=0)=\begin{cases}0 & 0<z\le 2.5\\ C_0 & 2.5<z<4.5\end{cases} \tag{S.5}$$

$$C(z,t=0)=C_0 \tag{S.6}$$

Analytical solutions are available for each of these cases (Crank 1975)[1]. The solutions for the control cell, 2.5-cm cap cell, and 4.5-cm cap cell are respectively:

$$C(z,t)=zC_0+C_0\sum_{n=1}^{\infty}\frac{2}{n\pi}\sin\left(\frac{n\pi z}{L}\right)\exp\left(-\frac{n^2\pi^2 D_{bio}t}{L^2}\right) \tag{S.7}$$

$$C(z,t)=zC_0+C_0\sum_{n=1}^{\infty}\frac{2\cos\left(\frac{2.5n\pi}{L}\right)}{n\pi}\sin\left(\frac{n\pi z}{L}\right)\exp\left(-\frac{n^2\pi^2 D_{bio}t}{L^2}\right) \tag{S.8}$$

$$C(z,t)=zC_0+C_0\sum_{n=1}^{\infty}\frac{(-2)^n}{n\pi}\sin\left(\frac{n\pi z}{L}\right)\exp\left(-\frac{n^2\pi^2 D_{bio}t}{L^2}\right) \tag{S.9}$$

Figure S.4 shows the behavior of these solutions at t = 0, 28 days, and infinity. Because of differences in initial conditions, the transient concentration profiles are expected to be different at 28 days although the steady state profiles are expected to be

the same for each cell. The differences between the model predictions are attributable to model error and natural variability observed between the microcosms.

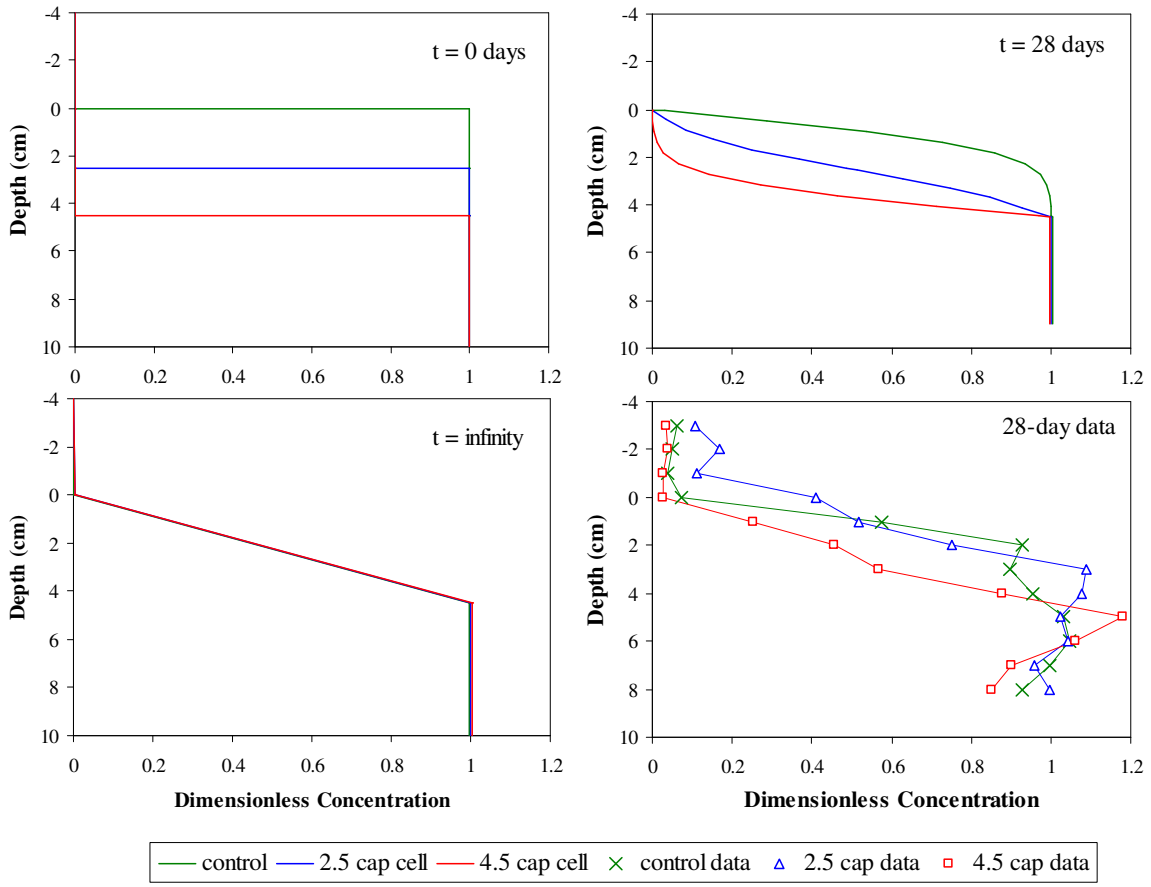

Figure S.4. Expected Behavior of Control, 2.5-cm, and 4.5-cm Microcosms at t = 0 days (upper left), t = 28 days (upper right), steady state (lower left), and the observed 28-day data (lower right).

References

1. Crank J. *The Mathematics of Diffusion*; Oxford University Press, London, 1975.